3-2002

IR-Based Estimation of Velocities Above Flames Spreading over Different Fuels

Lulu Sun
Embry-Riddle Aeronautical University, sunl@erau.edu

Xiangyang Zhou
University of California, Riverside

David R. Weise
USDA Forest Service - Pacific Southwest Research Station

Shankar Mahalingam
University of California, Riverside

Sun, L., Zhou, X., Weise, D.R., & Mahalingham, S. "IR-Based Estimation of Velocities Above Flames Spreading Over Different Fuels," Spring WSS/CI meeting of The Combustion Institute, San Diego, CA, March 25-26, 2002.

IR-Based Estimation of Velocities Above Flames Spreading over Different Fuels[1]

Lulu Sun[+], Xiangyang Zhou[+], David R. Weise[++], and Shankar Mahalingam[+]

[+]Department of Mechanical Engineering
University of California, Riverside, CA 92521

[++]Forest Fire Laboratory
4955 Canyon Crest Drive, Riverside, CA 92507

Paper # 02S-88 presented at the 2002 Spring Meeting of the Western States Section of The Combustion Institute, March 25-26, San Diego, CA

ABSTRACT: Wildfire spread in living vegetation such as chaparral in California and eucalyptus forests in Australia often causes significant damage to infrastructure and ecosystems. A physically based empirical model to predict fire spread rate is used in the United States to assist in a variety of fire management operations. The spread model does not adequately describe the chemical processes of combustion in live fuels.

Prior to describing and modeling the chemical processes of combustion in wildland fuels using computational fluid dynamics, we are investigating a technique to non-intrusively measure flame gas velocities using thermal imagery. By tracing "hot" pixels through successive digital images, we estimate velocity field using gradient-based algorithms. We also explore techniques established in digital particle image velocimetry (DPIV) to estimate fluid velocities. The images are acquired by a thermal camera with uncooled microbolometer 320×240 pixel focal plane array in the 7.5 - 13 μm spectral range. We estimated fluid velocities in flames spreading above isopropyl alcohol and shredded aspen wood (excelsior). Results from excelsior fires are presented. Finally, results obtained from computational modeling were used to validate the velocity field estimated from the gradient-based algorithm. Preliminary results using a DPIV-based algorithm appear promising.

INTRODUCTION

Wildfire spread in living vegetation such as chaparral in California and eucalyptus forests in Australia often causes significant damage to infrastructure and ecosystems. For predicting fire spread rate, existing models utilized by the Forest Service are based on the semi-empirical model developed originally by Rothermel (1972). It is applicable to quasi-steady burning of surface fires with uniform fuel loading and assumes that the fuel is dominated by dead material and in close proximity to the ground. Crown fire, transition from ground-to-crown-fire, fire spread through live fuels, fire spread by spotting, and modification of meteorological conditions by the fire are some of the phenomena not accounted for in the Rothermel model. Wilson (1982, 1985) examined fire spread in moist fuel and proposed changes in the manner in which moisture content is modeled in the Rothermel model. Wilson (1990) suggested that a term in the spread model involving wind and fuel moisture might be appropriate. However, the application of this to shrub fuel beds such as chaparral is currently unknown. Fuel depths observed in chaparral crowns range from 30 to 120 cm and vary by species, elevation, slope aspect, and rainfall. Total height of chaparral stands ranges from 1 to 6 m, and the crowns tend to be fairly porous (low packing ratio). In fact, fire spread in chaparral has been described as a crown fire. This provides the motivation to determine what is necessary to establish a propagating flame front in chaparral brush fuels independent of ground fuels.

Fire spread in wildland fuels is created by the coupled effects of fuel combustion, air convection, flame and ember radiation, and mechanical advection effects such as rolling embers and spotting. As an essential component of the convection, intense fire vortices on the scale of meters almost certainly play a fundamental role in the physics of fire spread (Emmons and Ying, 1967; Byram and Martin, 1972; Haines, 1982). McRae and Flannigan (1990) describe fire vortices that in one case were observed to rip out and loft standing trees. Clark et al. (1999) observed a fire vortex rising more than 3 km above ground level with flaming materials that were visible at about 2 km. Therefore, fire vortices not only are suspected of being hazards to nearby firefighters, but are an important fire spread mechanism through both local dynamics and the ability to loft flaming objects into areas well removed from the former fire front (Clark et al., 1999).

Because of the difficulty in measuring the velocity field of wild fire, there is no currently available data that describes the small temporal and spatial scale involved in the fire vortices that help to determine fire spread.

The focus of this paper is on the investigation of non-intrusive techniques for measuring flame gas velocities using high frequency, high-resolution radiant temperature images obtained by a thermal infrared camera. The velocity field that represents the motion of object points across an image is called the optical flow field. Optical flow results from relative motion between a camera and objects in the scene. In our method, the object points are represented by "hot" pixels measured by the thermal camera. One method is to trace "hot" pixels through successive digital images, to estimate vertical velocities The "gradient based algorithm" relies on an equation that relates optical velocities to spatial and temporal changes in the image (Lucas and Kanade, 1981; Kearney et al., 1987; Simoncelli et al., 1993, Clark et al., 1999). These gradient-based algorithms are generally relatively simple to implement, efficient to compute, and can produce accurate dense optical flow fields. For example, an empirical study by Barron et al. (1994) found the gradient-based local optimization method to be the best-performing overall. The general assumption in this algorithm is that the signal from a point on the object in space does not change with time and is therefore invariant with motion. In our case the signal from a point is the IR temperature that is assumed conserved over a short time required for analysis. An alternate method of estimating velocities is based on established techniques in digital particle image velocimetry (DPIV) (Willert and Gharib, 1991; Raffel et al., 1998). It is assumed that over small time intervals the signal of the hot pixel is conserved and behaves like a fluid particle analogous to seed particles used in an actual DPIV algorithm.

The fire plume experiments were completed using alcohol and shredded aspen wood (excelsior) as fuel. The fire images were acquired by a thermal camera FLIR SC500[2] with uncooled microbolometer 320×240 pixel focal plane array in the 7.5 to 13 μm spectral range. Results from a gradient-based algorithm to estimate fluid velocities in flames are presented. As a useful validation tool, a CFD (computational fluid dynamics)

[2] The use of tradenames is provided for informational purposes only and does not constitute an endorsement by the U.S. Department of Agriculture.

code was applied to simulate the fire plume for approximate conditions as in the laboratory experiments. The goal was to utilize predicted temperature fields to estimate fluid velocities using the two algorithms discussed, and to compare these estimates with simulation results. In this paper, the fire dynamics simulator (FDS) code developed by McGrattan et al. (2000) was used to compute the temperature and velocity field in the fire plume. The computed instantaneous temperature data were assumed as successive digital images. The gradient-based algorithm and the DPIV-based algorithm were used to estimate the velocity field. The gradient-based estimation of velocities were compared with that obtained by FDS code. Results illustrate the applicability and performance of gradient-based algorithms in fire research. Preliminary DPIV-based result although promising, requires further investigation.

GRADIENT-BASED ALGORITHM

The gradient constraint equation relates optical flow velocity on the image (u, w) and the image brightness function $\varphi(x, z, t)$, which corresponds to the temperature $T(x, z, t)$ obtained by experiment or computation (Clark et al., 1999). Here x and z denote horizontal and vertical coordinate directions in the image, with u and w denoting velocity components along these directions respectively. In our case the signal from a point is assumed conserved over a short time required for analysis. We assume the image motion is pure translation and its velocity components u and w are locally constant. So the governing equation for the image flow is

$$\frac{D}{Dt}\varphi = \varphi_t + u\varphi_x + w\varphi_z = 0 \tag{1}$$

It would be instructive to compare this equation to the energy equation of fluid flow under some certain circumstances where internal heat generation is absent. The viscous dissipation and thermal diffusion are negligible. These circumstances would be applicable to the flow with a very large Reynolds number as the limiting case of small viscous forces compared with inertia forces. These two equations could be considered fairly analogous. The gradient of the image signal is stationary (conserved) over the short time.

$$\frac{D(\nabla\varphi)}{Dt} = 0 \tag{2}$$

The images of fires are taken frame by frame from a stationary camera, frame 1 and 2, with the time difference, Δt. By assuming that fire particle motion is dominated by pure translation motion, each of the fire particles of frame 1 translates from pixel coordinate (x, z) to $(x+\Delta x, z+\Delta z)$ of frame 2. The function that we want to minimize is of the form,

$$\Lambda = \sum\left[\varphi_1(x+\Delta x, z+\Delta z) - \varphi_2(x,z)\right]^2 \tag{3}$$

where φ_1 is the temperature on the two-dimensional field at time t, and φ_2 is the temperature at time $t+\Delta t$. Summation is taken over all the pixels in the image. By Taylor series expansion approximation,

$$\varphi_1(x+\Delta x, z+\Delta z) = \varphi_1(x,z) + \Delta x\frac{\partial\varphi}{\partial x} + \Delta z\frac{\partial\varphi}{\partial z} \tag{4}$$

Substituting this in (3), the quantity Λ is minimized with respect Δx and Δz. This results in the matrix equation for the estimate Δx and Δz,

$$\begin{pmatrix} \sum\left(\frac{\partial\varphi}{\partial x}\right)^2 & \sum\left(\frac{\partial\varphi}{\partial x}\frac{\partial\varphi}{\partial z}\right) \\ \sum\left(\frac{\partial\varphi}{\partial x}\frac{\partial\varphi}{\partial z}\right) & \sum\left(\frac{\partial\varphi}{\partial z}\right)^2 \end{pmatrix}\begin{pmatrix}\Delta x \\ \Delta z\end{pmatrix} = \begin{pmatrix} \sum(\varphi_i - \varphi_{i,c})\frac{\partial\varphi}{\partial x} \\ \sum(\varphi_i - \varphi_{i,c})\frac{\partial\varphi}{\partial z} \end{pmatrix} \tag{5}$$

where the subscript i denotes the thermal images taken at different time levels and i,c denotes the center time image. Summations are taken over local paths of pixels. Once Δx and Δz at each pixel are calculated, velocity components u and w at each pixel can be calculated from

$$u = \frac{\Delta x}{\Delta t},\ w = \frac{\Delta z}{\Delta t}, \tag{6}$$

respectively.

DPIV-BASED ALGORITHM

The digital particle image velocimetry (DPIV) is an effective instantaneous and non-intrusive technique. It allows evaluation of the instantaneous velocity field by recording the position of seed particles at successive time images. The selected two (or more) sequential images are analyzed by subdividing the image into small interrogation areas (IA). In order to determine the displacement of seed particles, a statistical cross-correlation analysis algorithm is applied to each pair of small interrogation areas. This is given by,

$$\Phi_{fg}(m,n) = \sum_i \sum_j f(i,j) g(i+m, j+n)\,, \tag{7}$$

where $f(i,j)$ and $g(i,j)$ denote the image intensity distribution of the first and second image, m,n is the pixel offset between the two images and $\Phi_{fg}(m,n)$ is the standard cross-correlation function. When the offset values at which the IA's particle images align with each other, the sum of the products of pixel intensities will be larger than elsewhere, resulting in a high cross-correlation value Φ_{fg} at this position. The cross-correlation function is a statistically measure of the degree of match between the two IA's for a given offset, so the maximum value in an IA can be used to estimate the average particle displacement in the IA. This process is repeated for each area of interrogation over the two image frames, the result is a complete velocity vector field for the selected image.

An easy way to calculate the cross-correlation function (7) and obtain velocity vector field is explored. By using *normxcorr2* function included in *MATLAB* (The MathWorks, Inc.) software, the normalized cross-correlation function reads as follows:

$$\Phi_{fg}(m,n) = \frac{\sum_i \sum_j \left[f(i,j) - \bar{f}\right] \times \left[g(i+m, j+n) - \bar{g}(m,n)\right]}{\sqrt{\sum_i \sum_j \left[f(i,j) - \bar{f}\right]^2 \times \sum_i \sum_j \left[g(i,j) - \bar{g}(m,n)\right]^2}} \tag{8}$$

The result is the cross-correlation coefficient function, which modifies the standard cross-correlation function and gives better results. *Normxcorr2* function in *MATLAB* uses Fast Fourier Transform (FFT) based cross-correlation (FFT-CC) function instead of direct cross-correlation (D-CC) function. The difference between these two functions is that the discrete cross-correlation function is defined for a finite region, while the FFT-based cross-correlation function has to be extended to an infinite domain. FFT-based cross-correlation simplifies and significantly speeds up the evaluation process.

EXPERIMENTAL PROCEDURE

Experiments were performed on small pool fires in the middle of the fire laboratory, i.e., well away from aerodynamic obstacles. The small pool fires were contained in aluminum trays of horizontal dimensions 330×200 mm and depth 40 mm. The fuel used was alcohol and shredded aspen wood (excelsior). Chamise, one of several dominant shrubs in chaparral, will be used in the next experiment.

For the IR-based method, we used successive digital images captured by an infrared thermography camera, through tracing "hot" pixels to get velocity field. An infrared thermography camera can produce images of invisible infrared or "heat" radiation and provide precise non-contact temperature field. Successive images are captured from the ThermaCAM SC500 IR camera, which can provide optimal thermal sensitivity and non-contact temperature measurement precision where thermal differences are small or very high accuracy is desired. Temperature changes as small as 0.07 °C can be distinguished. The sampling rate of the thermal camera is 5 Hz. As will be seen later, this low sampling rate limits the accuracy of estimated velocities. ThermaCAM software is used to get 320×240 pixel temperature field. A default flame emissivity (ε) of 0.92 was used. Even though the flame emissivities were much lower than 0.92, the results presented here are not affected since all pixels in the image were assigned equal ε. At the separate points above the pool fire, temperatures were also measured by 24 gauge Type K thermocouples, which will be used to estimate ε for the various flames we are studying. An electrical scale was used to measure fuel mass variation with time. A heat flux sensor was used to measure the rate of heat flux. The thermocouple results, the heat flux sensor results and the electrical scale results are not included in this paper.

NUMERICAL SIMULATION

The Fire Dynamics Simulator (FDS) code developed by McGrattan et al. (2000) was used in the present simulation. FDS code solves a form of the Navier-Stokes equations appropriate for low-speed, thermally-driven flows of smoke and hot gases generated in a fire (McGrattan et al., 1994,1998).

An approximate form of the Navier-Stokes equations appropriate for low Mach number applications is used in the model of FDS. The approximation involves the filtering of acoustic waves while allowing for large variations in temperature and density.

This gives the equations an elliptic character, consistent with low speed, thermal convective processes (Mahalingam et al., 1990). The computation is treated as a Large Eddy Simulation (LES) in which the large scale eddies are computed directly and the sub-grid scale dissipative processes are modeled. The fire is represented by discrete Lagrangian particles (or thermal elements) that originate at burner (or solid surface) and release heat at a specified rate.

RESULTS AND DISCUSSION

Estimated Velocity from Experimental Data

Figure 1 illustrates two successive temperature images obtained by an infrared thermal camera with a frequency of 5 Hz and a resolution of 320×240 pixels. The IR images represent thermal data of the front of the fire plume over the fuel of excelsior. The x direction is along the horizontal and z is the vertical direction. Using a ratio translation, x and z correspond to the physical geometric position.

The gradient-based image flow analysis scheme was applied to this sequence of temperature images to derive the instantaneous velocity field. Figure 2 shows the estimated fire velocity vectors overlying the background IR temperature field. The IR temperatures cover the full 25°−500°C temperature range of the camera setting. For about the first 0.15 m above the fuel pool the thermal field was saturated because the IR temperature exceeded 500°C. In this region, the estimated fire speed is not accurate because the movement of the 'hot' pixels may not be observed. Above this region, the upward velocity vectors and rotating air are shown in figure 2. There is an accelerating central core in the fire plume with relative high turbulent velocities at the edge of the fire. This is consistent with the vortex observed at the left and the right edges of the fire plume. It is known that the fire vortex leads to strong radial inflow of ambient air into the core of the fire. The estimated peak value of vertical velocity is about 2 m/s.

Overall, the estimated velocity field using gradient-based algorithm appears reasonable. Because there is no independently measured velocity data, the accuracy of this method in the present fire case cannot be assessed. One problem is that the current sampling frequency of 5 Hz is too low to capture the successive change of the temperature image to a satisfactory accuracy. For the gradient-based algorithm, the main assumption is that the signal is conserved over a short time. However, as shown in figure 1, the change of the temperature between the two successive images is evident over a relatively long sampling time interval of 0.2 seconds. This certainly is expected to reduce the accuracy of the gradient-based algorithm. In the next section, the temperature data obtained from the FSD code will be used to analyze the effect of image sampling frequency on the accuracy of the gradient-based algorithm.

Estimated Velocity from CFD Data

Recent increases in computer power and the development in turbulence and combustion models make it possible for researchers to use CFD (computational fluid dynamics) code to study fire. With a CFD code, it is possible to provide full information on density, velocity, temperature and species concentrations. In this paper, the FDS (fire dynamics simulator) code developed by McGrattan et al. (2000) was used to simulate the fire plume under the approximate condition with the present experiment. Because there were no measured velocity data, the purpose of the FDS code was to utilize predicted temperature fields to estimate fluid velocities using the two algorithms discussed, and to compare these estimates with simulation results. The three dimensional computational domain is 0.8×0.6×0.8 m in size along the x, y and z directions respectively. The grid used is 81×61×81. The heat release rate per unit area is 615 kW/m^2. The ambient temperature is 25 °C. The computed instantaneous temperature data were assumed as successive digital thermal images. Both the gradient-based algorithm and the DPIV-based algorithm were used to estimate the velocity field. These velocity field predictions were then compared with that obtained by the FDS code.

Figure 3 illustrates the successive images of temperature field computed from the FDS code for the pool fire using the assumed heat release rate. The time difference is 0.00687 second corresponding to a data sampling rate of 145 Hz. Over this short time period, a minor upward movement of the temperature images can be observed, however, the shape of the temperature images is almost same without significant change. This means the gradient-based algorithm can use the assumption that the signal from a point is conserved over a short time.

Figures 4 (a) and (b) show a comparison of the velocity vectors computed from FDS code and that estimated from gradient-based algorithm, overlaying the background temperature field. Overall, both velocity fields compare well in the fire region. There are upward velocity vectors in the core region and minor rotating vortices at the edge of the fire plume. The peak value of instantaneous vertical velocity estimated by gradient-based algorithm is about 9 m/s, which is a little larger than that calculated by FDS code, 7 m/s.

As discussed earlier, the frequency of the thermal images is important for the accuracy of the gradient-based algorithm. At a height z = 40 cm, figure 5 illustrates the comparison of the vertical velocity profiles obtained from FSD code and from gradient-based algorithm using temperature images with different sampling rates. It is clear that the frequency of the sampled images will influence the results obtained from the gradient-based algorithm. For the present case, the best accuracy is achieved with images procured with a sampling frequency of 145 Hz. At smaller sampling time intervals or high sampling frequency, the movement of the temperature images is not evident so that the value of Δz obtained from equation (5) is not accurate. At low sampling rates, the assumption of conserved signal from a point over a short time may not be applicable. However, it should be pointed out that an acceptable sampling rate might depend on the domain size of the thermal images and the speed of the images. In the experiment of a wild fire examined by Clark et al. (1999), the domain size of the IR thermal image is 20×20 m and the time step used is from 0.1 s to 66 s. The results obtained were reasonable, showing two rising towers of hot, rotating air that were consistent with vorticity at the fire front undergoing enhanced vortex tilting.

Using successive temperature images obtained from FDS code (shown in figure 3), the DPIV-based algorithm was utilized to estimate the velocity field. In the present case, the temperature signal at each grid point is assumed as a hot pixel or tracer particle. For the two-dimensional image shown in figure 3, the grid size is 81×81, corresponding to 6561 hot pixels. The sequential images are analyzed by subdividing the image into small interrogation areas (IA) including 9×9 pixels or grid points. In order to determine the displacement of hot pixels, a statistical cross-correlation analysis is performed. The interrogation areas from successive images are cross-correlated with each other. The correlation produces a signal peak, identifying the displacement, Δx and Δy, that is the result of a velocity vector describing the average direction and speed of pixel displacement in each small IA. This process was repeated for each IA spanning the entire image.

Figure 6 shows the velocity vector field obtained using the DPIV-based algorithm. Because of the selected size of IA, 9×9 pixels, each velocity vector represents the average velocity in each IA, the velocity vector field shows a low density. Due to the presence of vortices, the movement of the flame plume appears irregular. This makes it difficult to detect velocity vectors through cross-correlation. In general most of velocity vectors are upward that are consistent with the results obtained from the FDS code. At the edge of the fire plume, there are leftward and rightward velocity vectors due to the vortical motion. Overall the estimated velocity vector field from the DPIV-based algorithm reflects the basic structure of the fire plume, but the results are still not very satisfactory. The peak velocity magnitude is about 2 m/s compared to 7m/s obtained from the FDS code. The main reason for this large discrepancy is attributed to the relatively low resolution of the whole image (81×81) which was divided into small IA's including 9×9 pixels for estimating the velocity field. The low density of hot pixels influences the normalized cross-correlation, and detection of the position of its peak value. An important difference between the DPIV algorithm and the present DPIV-based algorithm is that the signal generated by tracer particles is conserved optical intensity, but the temperature value represented by hot pixel will change with time. These preliminary velocity estimates produced by the DPIV-based algorithm requires further investigation.

CONCLUSION

The use of thermal infrared imagery to estimate flame velocities in wildland fires was investigated. Two methods were considered. The first one is a gradient-based algorithm that relies on an equation that relates optical velocities to spatial and temporal changes in the image. The second method utilizes techniques in digital particle image velocimetry. The gradient-based estimation of velocities compared well with that obtained by FDS code. The sampling rate of the thermal images is important for the accuracy of the gradient-based algorithm. Results illustrate the applicability and performance of gradient-based algorithms in fire research. Preliminary DPIV-based results although encouraging, requires further investigation.

While techniques utilizing infrared imagery to estimate velocities are promising, we need to increase the sampling rate in order to gather more accurate information. In the near future, we will have the capability to measure flames at sampling rates in excess of 30 Hz. The DPIV-based algorithm provides an easy and fast tool to implement FFT based cross-correlation to estimate fluid velocities. Additional improvements under investigation include acquisition of high-resolution images, three-point estimators, offsetting the interrogation areas to increase the matched "hot" pixels, etc. High-resolution imagery, coupled with gradient-based and DPIV-based algorithms enables us to estimate flame velocities in sufficient detail to enable comparison with computational models of combustion in live fuels.

ACKNOWLEDGEMENTS

The funding source for this research is the USDA Forest Service National Fire Plan administered through a Research Joint Venture Agreement No. 01-JV-11272166-135 with the Forest Fire Laboratory, Pacific Southwest Research Station, Riverside, CA. We thank W. Pakdee and Y. Khunatorn for their valuable technical input.

REFERENCES

1. Barron, J. L., Fleet, D. J. and Beauchemin, S. S. (1994). Performance of optical flow techniques, *Int. J. Computer Vision*, 12(1): 43-177.
2. Byram, G.M. and Martin, R.E. (1970). Modeling of fire whirlwinds. *Forest Science* 16(4): 385-399.
3. Clark, T. L., Radke, L., Coen, J. and Middleton, D. (1999). Analysis of Small-Scale Convective Dynamics in a Crown Fire Using Infrared Video Camera Imagery, *Journal of Applied Meteorology*, Vol. 38, pp 1401-1420.
4. Emmons, H.W. and Ying; S. J. (1967). The fire whirl. In *Eleventh Symposium (International) on Combustion*, pp. 475-486.
5. Haines, D.A. (1982). Horizontal roll vortices and crown fires. *J. Applied Meteorology*, 21(6):751-763
6. Kearney, J. K., Thompson, W. B. and Boley, D. L. (1987). Optical flow estimation: An error analysis of gradient-based algorithms with local optimization. *IEEE Trans. Pattern Analysis and Machine Intelligence*, 9(2):229-244.

7. Lucas, B. and Kanade, T. (1981). An iterative image registration technique with an application to stereo vision, In *Proc. 5th Int. Joint Conf. Artificial Intelligence*, pp. 674-679.
8. Mahalingam S., B. J. Cantwell and J. H. Ferziger, "Full numerical simulation of coflowing, axisymmetric jet diffusion flames," *Physics of Fluids A*, **2** (5), pp. 720-728, 1990.
9. McGrattan, K. B., Baum, H. R., Rehm, R. G., Hamins, A. and Forney, G. P. (2000). Fire Dynamics Simulator, Technical Reference Guide, *Technical Report NISTIR 6467*, National Institute of Standards and Technology, Gaithersburg, Maryland, January 2000.
10. McGrattan, K. B., Rehm, R. G. and Baum, H. R. (1994). Fire-Driven Flows in Enclosures, *Journal of Computational Physics*, 110(2): 285-292.
11. McGrattan, K. B., Rehm, R. G. and Baum, H. R. (1998). Large eddy simulations of smoke movement, *Fire Safety Journal*, 30:161.
12. Raffel, I. M.; Willert, C.E.; Kompenhans, J. (1998). Particle image velocimetry: a practical guide, Berlin: Springer.
13. Simoncelli, E. P. (1994). Design of multi-dimensional derivative filters, *In Proc. First IEEE Int. Conf. Image Processing*, vol. I, pp. 790-779.
14. Willert, C.E.; Gharib, M. (1991). Digital particle image velocimetry, *Experiments in Fluids* 10, pp. 181-193.
15. Wilson, R. A., Jr. (1982). Reexamination of Fire Spread in Free Burning Porous Fuel Beds, *USDA For. Serv. Res. Rep.* RP-289.
16. Wilson R. A., Jr. (1985). Observations of Extinction and marginal Burning States in Free Burning Porous Fuel Beds, *Combust. Sci. Tech.* 44:179-193.
17. Wilson, R. A., Jr. 1990. Reexamination of Rothermel's fire spread equations in no-wind and no slope conditions. *USDA For. Serv. Research paper INT* 434, Ogden, UT, p. 13.

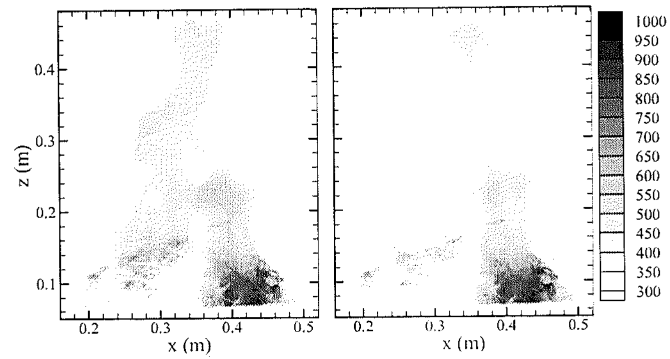

Figure 1. Successive images of temperature (K) field of the pool fire above the fuel of excelsior measured by thermal camera with time difference 0.2 s or sampling rate 5 Hz.

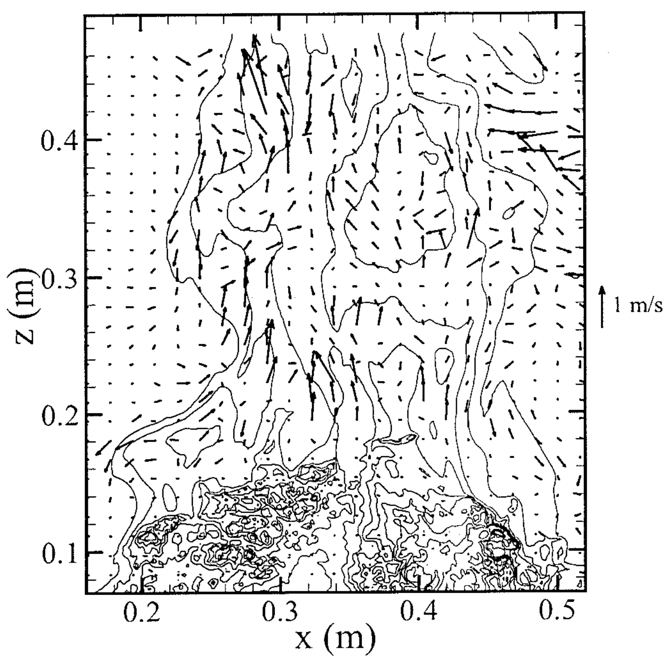

Figure 2. Velocity vector field estimated by the gradient-based algorithm from the thermal images shown in figure 1, overlying the background IR temperature field.

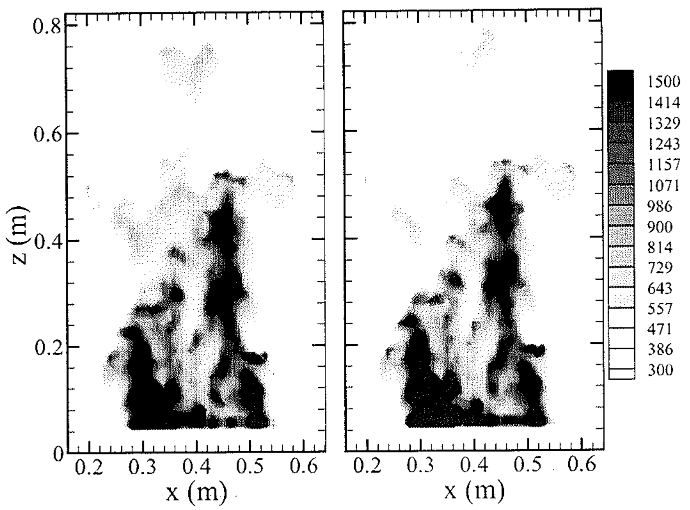

Figure 3. Successive images of temperature (K) field calculated from the FDS code for the pool fire with a sampling rate 145 Hz.

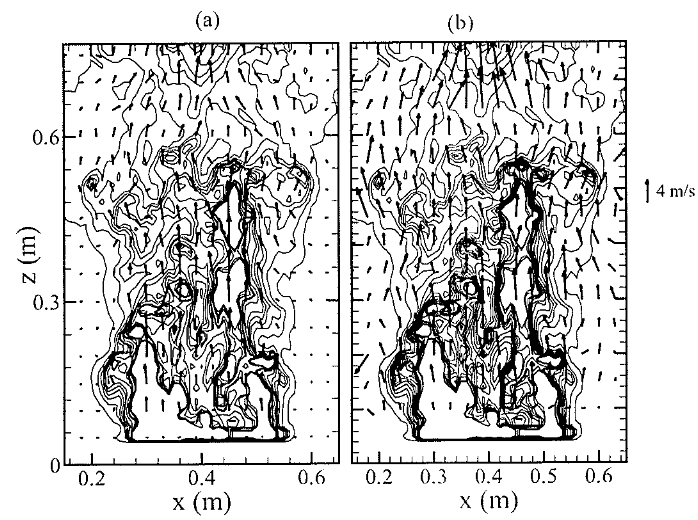

Figure 4. Comparison of velocity vector field (a) computed from FDS code; (b) estimated by gradient-based algorithm using temperature images obtained from FDS code. Sampling rate is 145 Hz. Temperature contours are illustrated to show the flame shape.

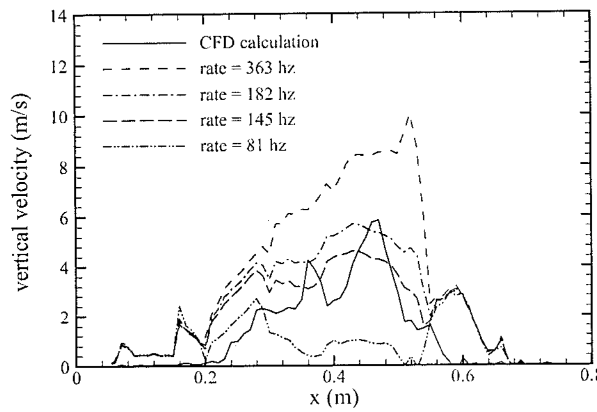

Figure 5 Comparison of instantaneous vertical velocities (at $z = 0.4$ m) computed by FDS code and estimated by gradient-based algorithm with different image sampling rates.

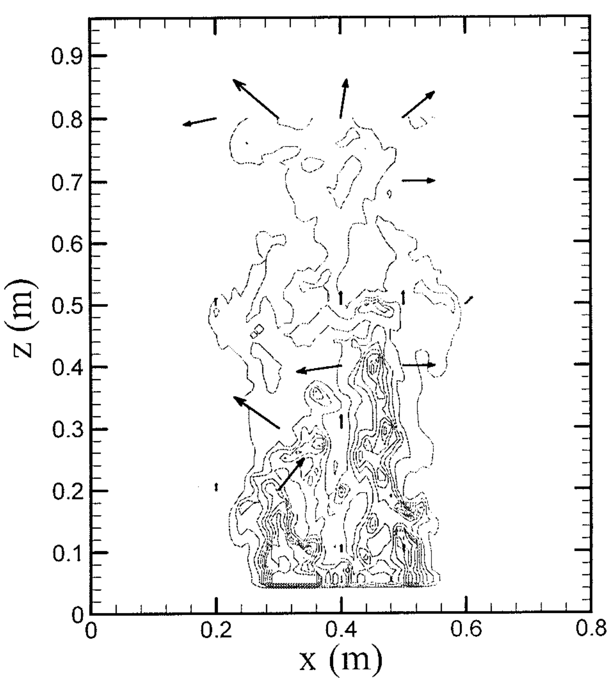

Figure 6. Velocity vector field estimated by DPIV-based algorithm using two successive images calculated from FDS code with image sampling rate 145 hz.